WIND TUNNEL TESTING OF POROUS DEVICES FOR THE REDUCTION OF FLAP SIDE-EDGE NOISE

F.M. Catalano*, P. Vanuchi* and L.G.N. Correa**
***Laboratory of Aerodynamics EESC-USP Brazil, **EMBRAER**
catalano@sc.usp.br; paulo.vanucci@gmail.com; luizguilhermecorrea@gmail.com

Keywords: *flap side edge noise, high lift wing.*

Abstract

This work investigates experimentally several flap side-edge treatments on a MD 30P30N wing model for noise reduction. The application of porous edges of various extensions, splitter plate were among the investigated treatments. The experiments were carried out in a solid wall low speed wind tunnel with turbulence level of 0.2% and capability of aeroacoustic testing with an overall SPL at 37m/s from 500 Hz to 20 kHz of 80 dB , with a peak 1/24 octave-band level of 75 dB at 500Hz that decreases to 67 dB at 2 kHz. The baseline configuration and those with side-edge treatments were tested and equivalent noise levels were obtained for low frequencies. For higher frequencies, the model with porous plates has a lower noise level, reaching a difference of 6 dB in 3.2kHz, compared to the baseline configuration.

1 Introduction

High lift devices, and landing gears, are the main sources of airframe noise during the approach and landing phase of aircraft flight. High lift devices include leading edge slats and trailing edge flaps. At slat cove region there is flow separation, flow recirculation, an unsteady shear layer, and slat settings together generate noise of mainly broadband content. For a flap, the outboard flap side edge and vortex system associated with it are the main sources of noise. The intensity of high lift device noise generally follows a power law of flow velocity. The noise that is generated at the side edge of the flaps has been identified as an important airframe noise component and is a target for noise control. A number of numerical and experimental studies have been conducted in order to identify and model the noise generation mechanisms at the flap side edge. Flow field measurements [1] in the flap side edge region of a wing with a half-span flap have revealed the presence of a 2-vortex system (Fig. 1): a small vortex near the flap side edge on the top surface and a stronger side vortex along the lower portion of the flap side edge. As it travels downstream along the flap side edge, the side vortex strengthens and expands (F to D at Fig. 1). At about mid-chord it begins to spill over the flap top surface and merges with the small top vortex (C to B). The instabilities in this vortex system and in the strong shear layer that originates on the bottom edge of the flap create an unsteady pressure field at the flap side edge causing sound to radiate. Brooks et al. [2] have determined that the dominant flap side edge noise regions are located around mid-chord on the pressure side of the flap edge and around 60-65% chord on the suction side.

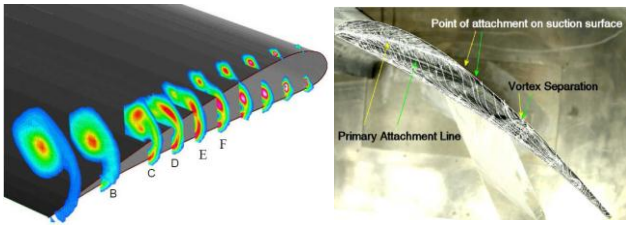

Fig. 1 Flap side edge vortex formation from flow measurements [1] oil flow and calculations [3].

Angland [3] conducted an experimental and computational investigation to determine the aerodynamics and aeroacoustics of flap side-edge. A porous treatment to the flap side edge was applied in an attempt to reduce noise of the flap edge. Measures taken in the experimental

study were forces, surface pressures, particle image velocimetry, hotwire anemometry and surface microphones. Oil flow was performed to visualize the flow on side edge surface. From the experimental and computational investigation four sources of vorticity in the flow-field were identified, at the main element cove, the main element trailing-edge, flap separation, and the flap side-edge vortical system. These sources of vorticity interacted to produce a significantly unsteady flowfield above the solid flap surface and noise. The application of a porous flap side-edge reduced the magnitude of vorticity in the turbulent shear layer and the vortex with a consequent less hydrodynamic instability at the flap side-edge. This work is an aerodynamic and aeroacoustic measurement of the effect of side edge application o perforated plates.

2 Experimental Set-up

2.1 Wind Tunnel

The LAE-1 closed circuit wind-tunnel was designed originally as a 3/8 scale pilot wind-tunnel of a proposed automotive wind-tunnel to be constructed. The wind-tunnel construction started on 1998 and finished in 2002, its predominant construction material is the naval plywood. With the automotive industries reduction of investments and the rebirth of the Brazilian aeronautic industry this wind-tunnel became a multi task wind-tunnel with instrumentation mainly focused on aeronautical tests for industry and academic researches.

The Fig. 1 presents a plan view of the LAE-1 closed circuit wind-tunnel. The wind-tunnel test section dimensions are 3.00 m long, 1.30 m high and 1.70 m wide. The maximum design flow speed is 50 m/s, with a turbulence level of 0.25%, nowadays due to safety and components long range issues, this velocity is limited to 45 m/s. Its electric motor, with 110 HP, drives an 8 blades fan with 7 straightners localized downstream the fan. On the flow stabilization section there are two mesh screens 54% porosity following by the 1:8 contraction cone designed using two 3rd order polynomials joined at 45% inflection point.

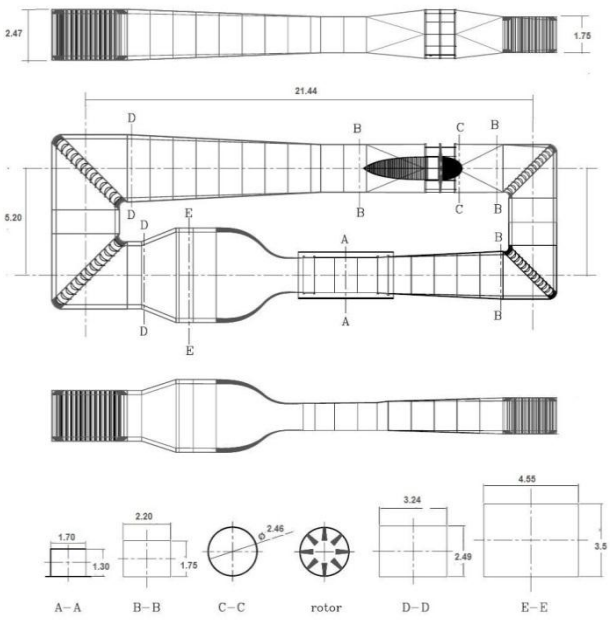

Fig. 1 Plan view of the LAE-1 wind-tunnel.

It is remarkable to mention the relative low turbulence level considering the installation of only two screens, and no honeycomb. These standards were only obtained due to the care taken during the design of low angle diffusers, low-drag corner-vanes and high-efficiency propeller blades designed with a combination of CFD and semi-empirical techniques. The meticulous construction of this wind-tunnel was also a key factor for its performance, fact that could explain the four years expended for its conclusion. More details about the design and construction of this wind tunnel can be found on **Erro! Fonte de referência não encontrada.**. Recently, the LAE-1 wind tunnel passed to an upgrade to reduce the background noise in order to carried-out beam-form noise measurements. Details of this upgrade and characterization can be found in [6] but Fig. 2 shows the final results for the wind tunnel background noise after the modifications. Fig 2 presents the Overall Sound Pressure Level (OSPL) variation with the flow speed. From Fig. 2 it is remarkable that the first phase of noise treatment reduced the OSPL in an average value of 4 dB for all flow velocities. In other hand the second phase of noise treatment reduced the OSPL just for flow velocities below 20 m/s, and had no effect for high velocities

flows. It can be explained by the fact that this treatment has reduced the noise for high flow velocities at high frequencies (frequencies of interest).

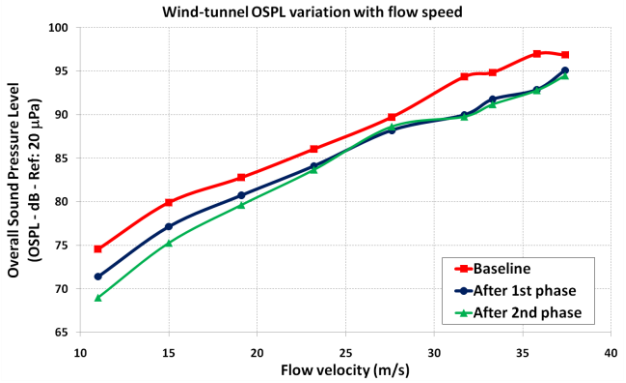

Fig. 2 OSPL variation with the wind-tunnel flow speed [5].

2.2 Two-dimensional testing

Testing two dimensional models altogether with aeroacoustic is a good way to find particular noise sources and at same time its physical explanation. However, two-dimensional aerodynamic testing has a main concern in guarantee a true two-dimensional flow over the model and this is not always a zero noise procedure. In fact, end-plates, split plates and wall-to-wall experimental set-ups used for guarantee two-dimensional flow, can generate as much as noise than trailing edges, separations etc. The unavoidable interference between the wings upper surface low pressures with the plates generate a secondary vortex that create noise. If the wing model has an airfoil of small C_{Lmax} (such as for symmetrical airfoils with less than 12% thickness) and aspect ratio greater than 9, these effect can be neglected. But, again, this is not the kind of practical situation for a wing of a standard aircraft at landing or taking-off even if no high lift devices are in place. What is more likely is a wing with C_{Lmax} higher than 2.0 with at least one high lift device (slat or flap). Testing high lift two-dimensional wing section is only possible if a control of the interaction between the wall boundary layer and upper surface flow is performed. There are two ways to control this interaction: tangential blowing and wall boundary layer suction. Both methods produce noise although; tangential blowing can generate more intense high frequency noise and should be avoided. A two-dimensional experimental set-up without any wall boundary layer control will produce wrong results and should be avoided as reference data for both aerodynamic and aeroacoustic. Even for low incidences, an HLW (high lift wing) will produce strong horse shoes vortices that will induce not only a tri-dimensional flow over the surfaces but also extra noise. Figure 3 shows a schematic demonstration of the horse-shoe vortex formation between a wing and a wall boundary layer. Previous experiment set-up developed at LAE/EESC-USP in order to assure two-dimensional high-lift testing used suction at discrete areas near the upper surface of a wing model with slat and flap. The idea was to remove the wall boundary layer before it separates and create a horse shoe vortex. The Figure 4 shows the wall-to-wall wing model attached to two turn tables where suction was promoted.

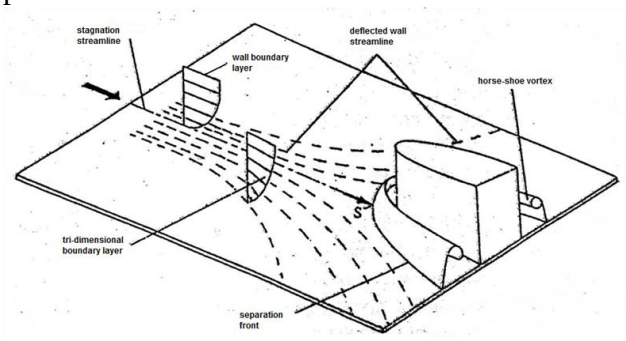

Fig. 3 Horseshoe vortex formation between a flat plate and a wing with circulation.

Fig. 4 High lift experimental set-up with wind tunnel wall boundary layer suction.

The model had various pressure tapping rolls: one central which include flap and slat; two in

the main element only located near the roof and floor; one spanwise distribution located at 1/4chord. Those pressure distributions was strategic located for checking up the effect of suction on sustain two-dimensional flow over the wing. Figure 5 show some results for incidence angle of 12 degrees. It is clear from Figure 5 that the effect of the wall boundary layer interaction with the wing flow must be controlled and this control can be carry-out by discrete suction although its effect is highly dependent on the suction mass flow. Figure 6 shows the effect of the suction mass flow over the spanwise pressure distribution at 1/4chord position. It can be seen that there is a minimum suction mass flow that guarantees two-dimensionality. Increasing suction mass flow will generate more noise which is not acceptable for aeroacoustic experiments. Therefore, for a quiet suction system a minimum suction mass flow should be set in order to assure both two-dimensional flow and generate minimum noise. Also clear that to assure two-dimensional flow on the slat and the flap is necessary less suction mass flow than for the main element. In this sense, optimizing the suction area for each section may lead to smaller suction mass flow and, therefore, less noise. In conclusion, there is no sense on two-dimensional HLW testing without any boundary layer control.

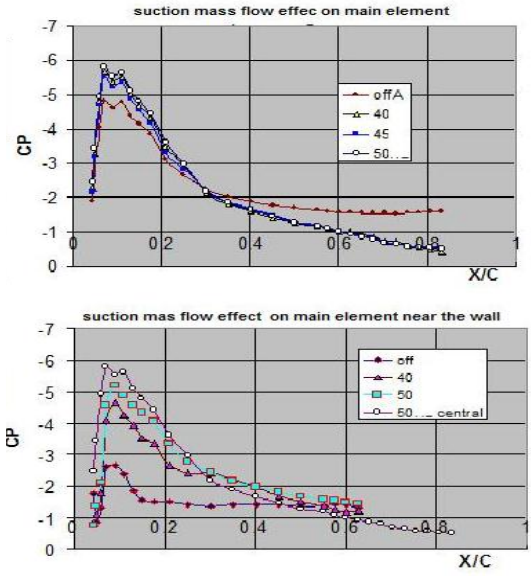

Fig. 5 Results for various suction mass flow on pressure distribution of a HLW.

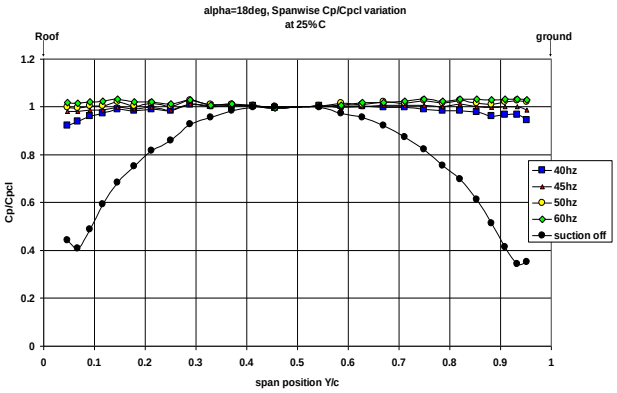

Fig. 6 Spanwise effect of wall boundary layer suction.

2.3 Wing model.

The wing model used for the experiments was the 30P30N. It is a three element, high lift configuration composed of a slat, main element and flap. The numerals contained in the model name represents slat and gap deflection angles (30 degrees each), respectively. The model has a span of 1.30m and a chord of 0,50m with the high lift systems stowed. The wing model spans the wind tunnel height and is attached to the same turn tables described previously which provides boundary layer suction to assure two dimensional. The 30P30N model is composed with a full span flap and a half span flap, Fig. 7 shows the model geometry and Fig. 8 shows the model installed at the wind tunnel test section with the full flap and with the half span flap.

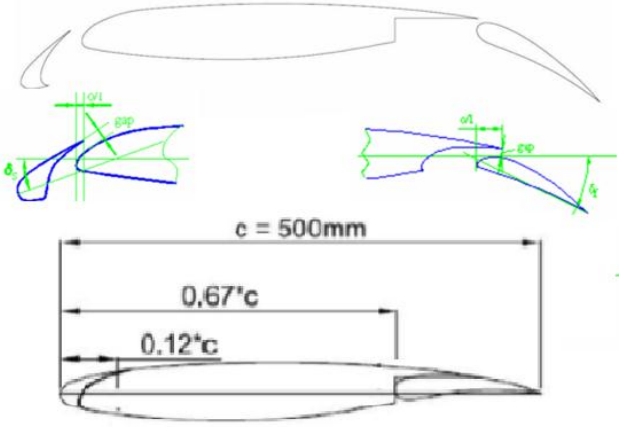

Fig. 7 30P30N model geometry.

Fig. 8 Wing model installed in the testing section.

2.4 Pressure measurements

Pressure measurements were carried out using a scanivalve® ZOC with a pressure transducer of ±2,5psia with an accuracy of ±0,10% of full scale. The slat and flap had each one 27 pressure taps distributed on both surfaces and the main element had 57 and 53 on the upper surface and bottom surface respectively.

Surveys of the wing wake and flap side edge were done with a low cost seven holes Pitot probe developed at the laboratory, using piezoresistive pressure transducers sensortechnics HCLA 12X5B of ±12,5mBar with accuracy of 0.05% to 0,25%FS. This probe was calibrated with 14 neural networks to measure flows with high angularity and it is especially suitable to obtain the flow field characteristics of the flap side edge vortices. Mapping was performed using a Dantec traverse gear with ±0,1mm accuracy.

2.5 Aeroacoustic measurements

For aeroacoustic tests, an array with 109 microphones was employed to measure noise sources intensity and location, using a beamforming technique. The antenna has 60 high frequency microphones suitable for acoustic measurements up to 40 kHz and 49 for measurements up to 16 kHz. Phased array signal processing using DAMAS2 algorithm was used to amplify the signal from the noise source under investigation and to attenuate the response to sound from other directions. Beamforming spectra were then obtained considering only the side-edge region.

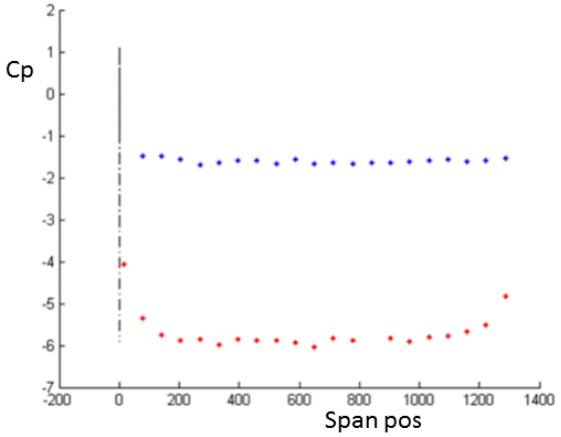

Fig. 9 Spanwise pressure distribution with wall suction.

3 Test Conditions and Configurations Studied

All the aerodynamic and aeroacoustic testing were conducted at average Reynolds number of $1x10^6$ unless for the side edge mapping and aeroacustic measurements where the Reynolds number was set at $8.4x10^5$. For all the spectral graphics of the project DAMAS2 algorithm was used, always with 1/12 octave step.

The NRT applied to the side edge are mainly porous plates of 33% porosity with holes of 0,75mm diameter and 1mm thickness. Table 1 shows the configurations tested where are also included a solid plate and a split plate. Figures

10 to 12 show the baseline and the flap side edge with porous plates and solid plates.

Table 1 Side edge attachments tested.

Test Number	Type Of Experiment	Location	Incidence Angle
16	Baseline		12º
17	Porous plate	Flap side edge bottom surface	12º
18	Porous plate	Flap side edge bottom and upper surface	12º
19	Porous plate	Flap side edge bottom surface (bigger plate, 15mm)	12º
20	Non porous plate	Flap side edge upper surface (bigger plate, 15mm)	12º
21	Split plate	Flap side edge	12º

Fig. 10 Test configuration 16 and 17.

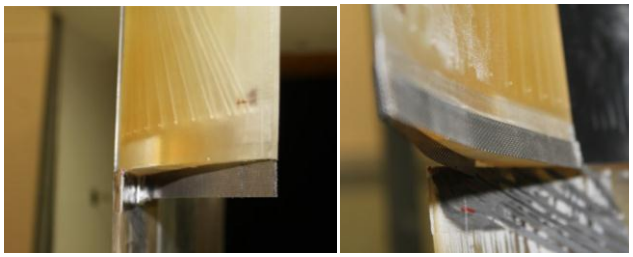

Fig. 11 Test configurations 18 and 19.

Fig. 12 Test Configuration 20 and 21.

Those configurations were designed for practical application in flap side edge of both new and old aircrafts. The metallic perforated plate is easy to be applied at one of flap surface without complex modification and could easily be certified.

4 Results and Discussion

4.1 Pressure Results

The pressure distribution sowed in here had two objectives: first to assure that the test conditions could be reproduced by CFD/CAA codes in order to be used as calibration data for those codes; secondly the pressure distributions were compared with previous results in order to access Reynolds number effect, transition and turbulent separation fronts. The second objective is not addressed in this work. Also was checked the minimum suction rate at the wind tunnel wall boundary layer control to assure two-dimensional flow at the model and the related effect at chordwise pressure distribution. Figs 13 and 14 show the results for suction on and off effect on pressure distribution for the wing model at 4^o. Also is plotted in Figs 13 and 14 the results for CFD calculations.

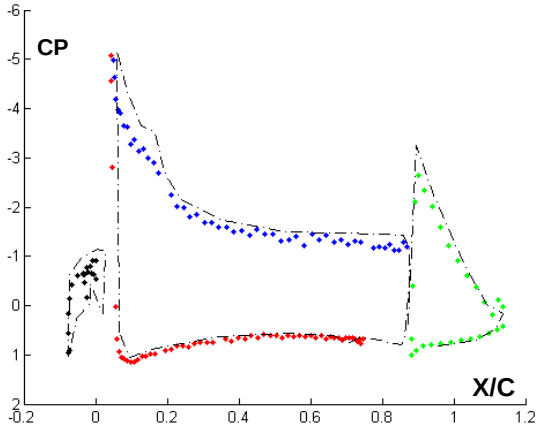

Fig. 13 Pressure distribution for $\alpha = 4^o$ suction off.

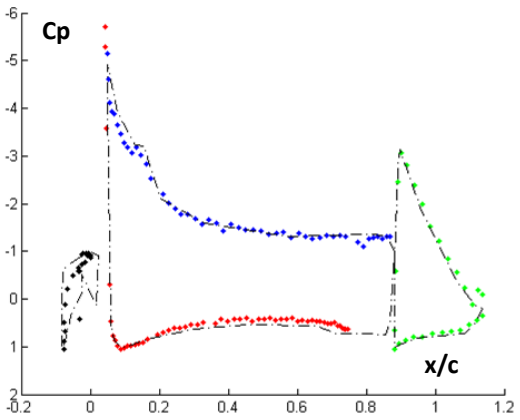

Fig. 14 Pressure distribution for $\alpha = 4^o$ suction on.

The following figures 15 and 16 show the results for incidence angle 16° with and without suction. It can be seen from Figs. 15 and 16 that the suction is more important than for 4° as the high suction peek interact strongly with the wind tunnel wall boundary layer generating the horseshoe vortex which promotes tri-dimensionality. As a consequence of that is noisier suction flow at the walls which could interfere with the aeroacoustic measurements. However, as we will note in the following results, the side edge vortex is also stronger producing more noise compensating the extra cumulative noise from the suction system.

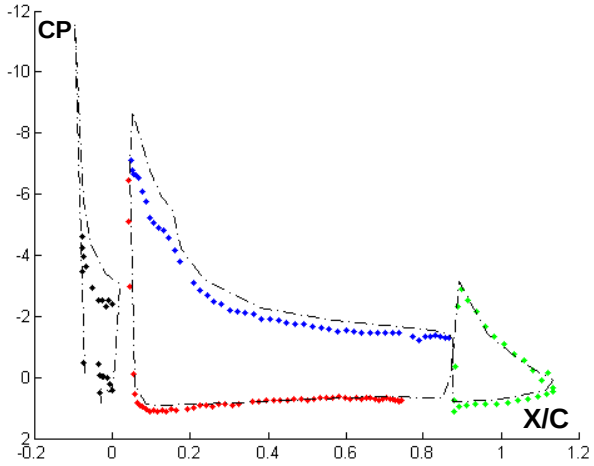

Fig. 15 Pressure distribution α=16°, suction off.

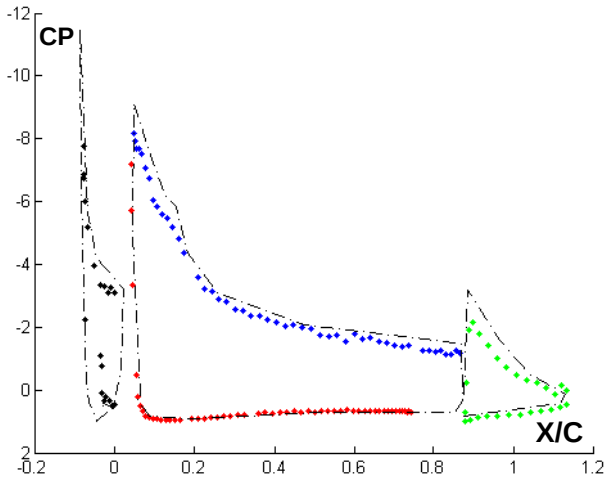

Fig. 16 Pressure distribution α=16°, suction on.

Figure 17 show the results for α=16° for the wake and downwash angle acquired from the measurements using the seven hole probe. The results presented in Fig. 17 were used for calculation of the profile drag and to check if there is enough suction to avoid three-dimensional flow. Variation on downwash can be an indication of three-dimensional flow as it can be seen in Fig. 18 were the effect of the horseshoe vortex at both wing end induces a three-dimensional downwash decreasing and moving downward the wake.

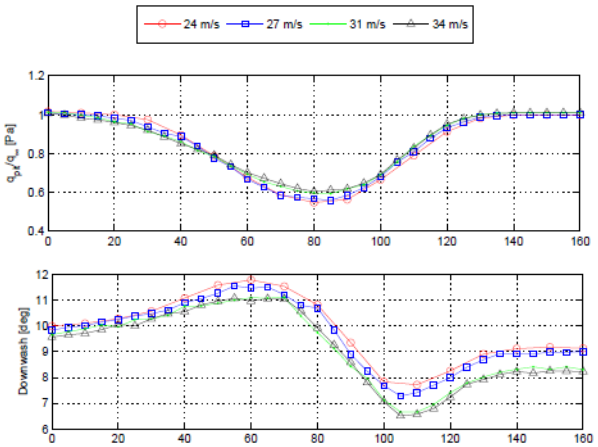

Fig. 17 Wake and downwash angle measured at 1.5chord downstream.

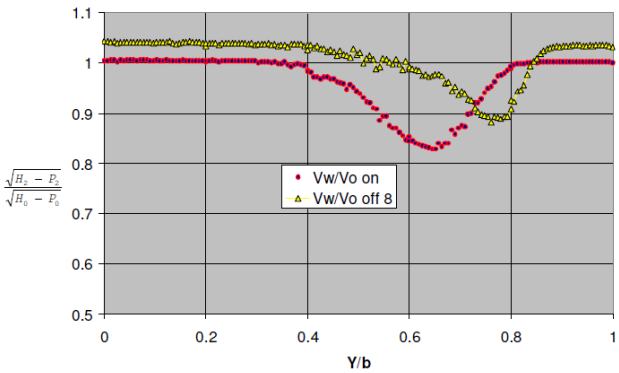

Fig. 18 Wake for α=8° with suction on and off.

It is important to avoid the horseshoes vortex near the wall because even for the tests with the flap side edge which is a three-dimensional flow, the absence of suction would induce a different vortex location and intensity and certainly would modify the aeroacoustic results.

4.2 Aeroacoustic results.

Conventional beamform and the DAMAS2 algorithm was used for all spectrum results and in order to compare the spectrum of all cases a region of interest (ROI) was defined as shown in Fig. 19.

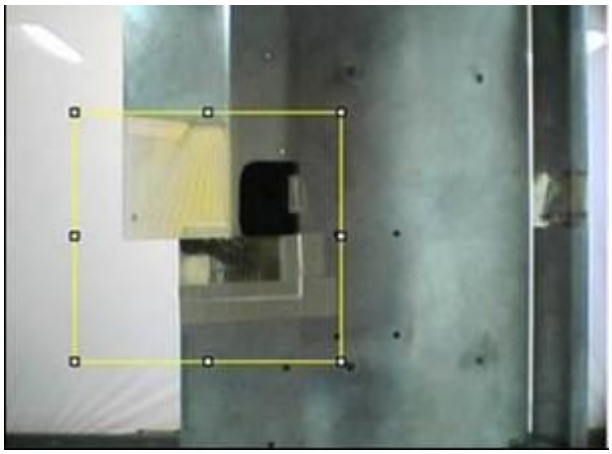

Fig.19 Region of interest

Figure 20 show the results of all side-edge attachments compared with the baseline case run 16. It can be noted in Fig. 20 that noise damping starts at 2.0 kHz for most of the porous attachment and as expected, it is a function of the perforated plate area as the effect is better for the case 19 which perforated strip is 10mm wider.

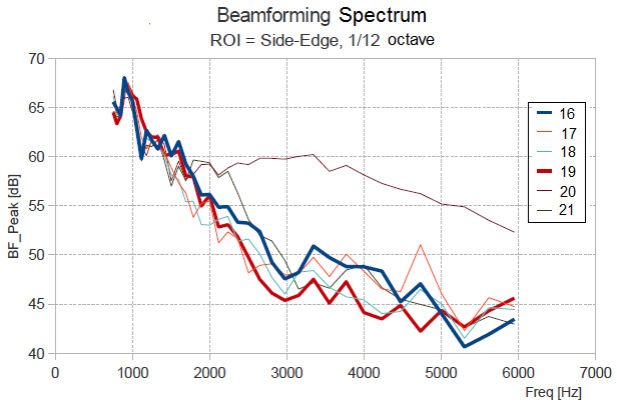

Fig. 20 Beamforming spectra calculated at ROI for the configurations tested.

Figure 21 show only the results for the baseline case compared with the case 19 without applying the ROI. From Fig 21 it can be seen that the broadband hump after 3.0 kHz is decreased up to 6db. Although, it is difficult to put numbers in noise level due the experiment been carried out in a non-anechoic working section the evidence in the decrease of the hump after 3kHz may be considered a positive effect.

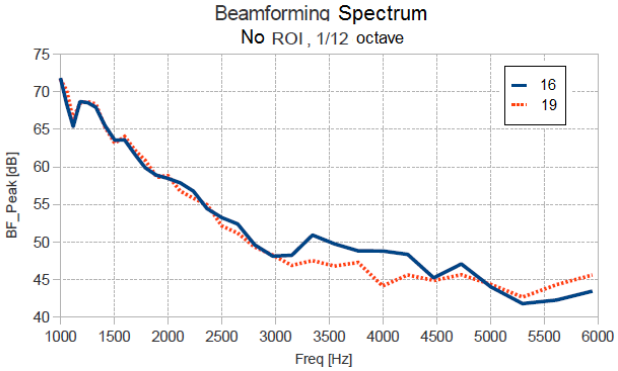

Fig. 21 Noise spectra for case 19 compared with the baseline.

Figures 22 and 23 show the beamform plots for the baseline and for the case 19. It can be seen from these results that besides reducing overall noise there are a change of the noise source locus probably due to an interaction of perforated plate and the main element.

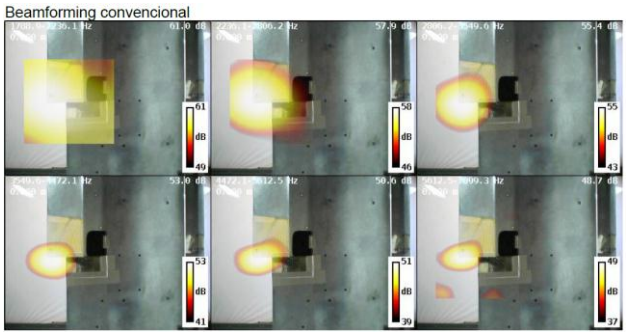

Fig. 22 Conventional beamform plots for the baseline case.

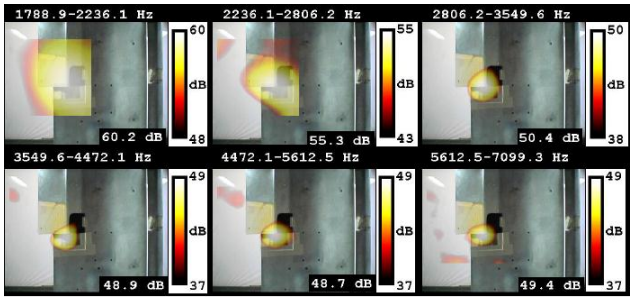

Fig. 23 Conventional beamform plots for the case 19.

Figure 24 shows the beamform results for only two frequency range for the baseline and case 19 applying the DAMAS2 algorithm. From Fig. 24 is even more evident the reduction of side edge source and its locus which was moved upstream. As pointed out before this shift of the noise source locus may be related with an aerodynamic interference between the perforated plate and the main element trailing edge. However, one of the effects of attaching porous material at the side edge is to move the vortex away of the local flap upper surface and this also can change the source locus.

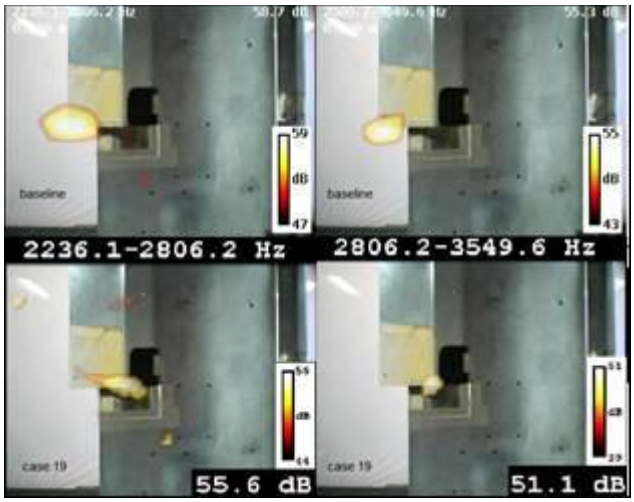

Fig. 24 Beamform maps comparison between the baseline and case 19.

The perforated plate used in this work is a different material than the foam used in [3] and although the general effect is similar in reducing the vortex intensity and also displacing it way from the flap edge surface it may introduce an extra effect related to the potential effect on acoustics. Perforated plate is specifically used in combustion chambers and it may have a strong influence on the acoustics of the chamber. Notably they may modify the acoustic modes of the chamber, and so have an influence on combustion instabilities. This effect is particularly important to keep the combustion through the chamber at constant velocity. In this work the flow passing through the perforated edge induced by the pressure difference at the flap edge may modify the acoustic modes of the flap side edge besides damping de vortex strength due to the local total pressure drop. The total pressure loss induced by the presence of the perforated plate was measured by the vortex mapping using the seven hole probe. The grid for mapping was generated in order to cover the vortex and both flap and main element wakes. Also, a denser grid was defined at the vortex core for precision.

Figure 25 shows the result of the mapping and the grid position.

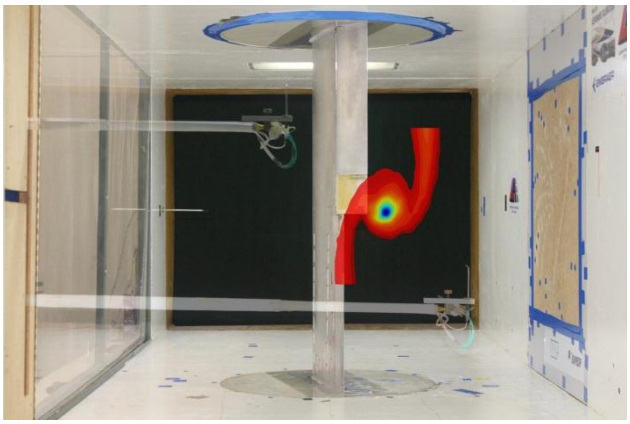

Fig. 25 Vortex and wake mapping , α=12°.

The Figs. 26 and 27 show the total pressure mapping at the vortex and wakes. It is clear the reduction of the total pressure when configuration 19 is used. This confirms the comments pointed out before relating pressure drop with noise reduction at the side edge.

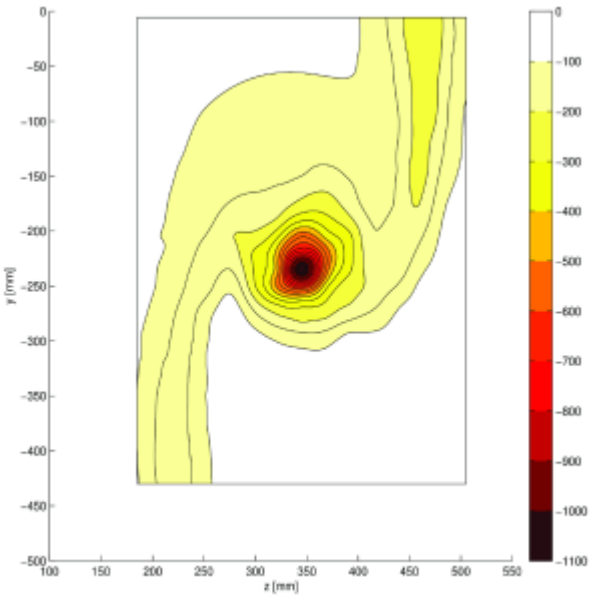

Fig. 26 Total pressure drop mapping of the vortex and wake, Baseline case.

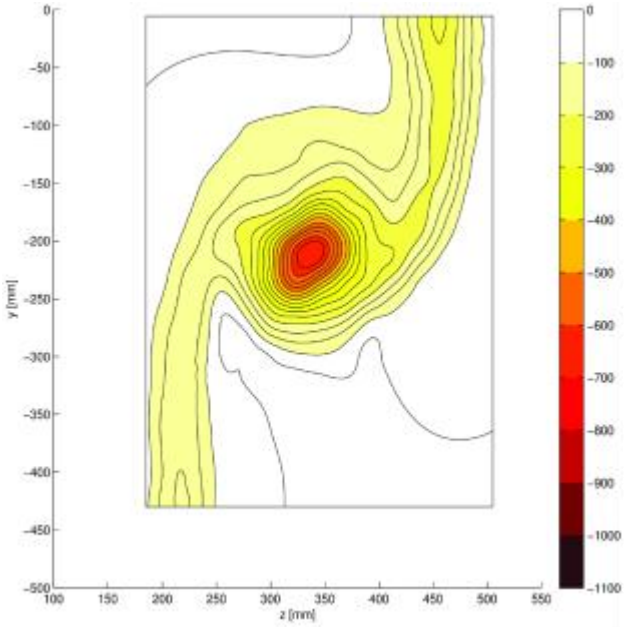

Fig. 27 Total pressure drop mapping of the vortex and wake, case 19.

5 Conclusions

An experimental work was carried out in order the test the application of perforated plates at the flap side edge of a high lift wing. Aerodynamic and aeroacoustic analysis was performed altogether to identify noise sources at the flap side edge and aerodynamic explanations. The positive effects of the application of perforated plate at flap side edge on the nearfield flow were to reduce the strength of the vortex and the shear layer that fed vortex. Another favorable effect was the displacement of the vortex away from the surface. The flow passing through the perforated edge induced by the pressure difference at the flap edge may modify the acoustic modes of the flap side edge besides damping de vortex strength due to the local total pressure drop. It could be found that noise damping starts at 2.0 kHz for most of the porous attachment and as expected, it is a function of the perforated plate area. The pressure drop imposed by the perforated plate decrease the vortex strength and its position relatively to the baseline model. The potential use of a metallic perforated plate as a noise reduction technology is considered good as it will not require great modifications in the flap side edge and could be easily certified.

6 References

[1] Radezrsky, R. H., Singer, B. A. and Khorrami, M. R., Detailed Measurements of a Flap Side-Edge Flow Field, AIAA Paper 98-0700, 1998.

[2] Thomas F. Brooks, William M. Humphreys Jr. Flap-edge aeroacoustic measurements and predictions, Journal of Sound and Vibration 261 (2003) 31–74.

[3] David Angland, Aerodynamics and Aeroacoustics of Flap Side-Edges. PhD Thesis Faculty of Engineering, Southampton University February 2008

[4] H.M.M. van der Wal and P. Sijtsma Flap noise measurements in a closed wind tunnel with a phased array NLR-TP-2001-632

[5] Catalano, FM. “The new closed circuit wind tunnel of the aircraft laboratory of university of São Paulo”. 16th Brazilian Congress of Mechanical Engineering. Vol.6, pp 306-312,2001

[6] Leandro Santana, Fernando M. Catalano, Marcello A. F. Medeiros, Micael Carmo, The Update

[7] Process and Characterization of the São Paulo University Wind-Tunnel for Aeroacoustics Testing. 27th ICAS Nice France 2010.

[8] Ennes Sarrad and Thomas Geyer, Noise Generation by Porous Airfoils 13th AIAA/CEAS Aeroacoustics Conference (28th AIAA Aeroacoustics Conference) AIAA 2007-3719.

7 Acknowledgements

The authors acknowledge FAPESP and EMBRAER for the financial support for this project.

Copyright Issues